IJE TRANSACTIONS B: Applications Vol. 36, No. 02, (February 2023) 215-225

International Journal of Engineering

Journal Homepage: www.ije.ir

Artificial Neural Network-based Fault Location in Terminal-hybrid High Voltage Direct Current Transmission Lines

A. Hadaeghi*[a], M. M. Iliyaeifar[a], A. Abdollahi Chirani[b]

[a] *Department of Electrical Engineering, Ahrar Institute of Technology and Higher Education, Rasht, Iran*
[b] *Department of Electrical Engineering, University of Guilan, Rasht, Iran*

PAPER INFO

Paper history:
Received 11 March 2022
Received in revised form 15 November 2022
Accepted 16 November 2022

Keywords:
Fault Location
High Voltage Direct Current
Hybrid-High Voltage Direct Current
Artificial Neural Network
Wavelet Transform

ABSTRACT

In this article, a fault location technique based on artificial neural networks (ANN) for Terminal-Hybrid LCC-VSC-HVDC has been assessed and scrutinized. As is known, in conventional HVDC systems (LCC-based and VSC-based HVDCs), the same type of filter is used on both sides due to the use of similar converters in both sender and receiver terminals. In this article, it is concluded that due to the use of two different types of converters at the both ends of the utilized Terminal-hybrid LCC-VSC-HVDC system, and the use of different DC filters on both sides, fault location using positive and negative pole currents of the rectifier side has much better results than the rest of input signals. Therefore, it will be finalized that by increasing and designing suitable DC filters on the transmission line of HVDC systems, fault localization matter will be remarkably and surprisingly facilitated. Nowadays, the fault location of HVDC transmission lines with a value of more than 1% is generally discussed in most articles. In this research, the fault location with a value of 0.0045%, i.e., a distance of 22.5 meters from the fault point in the most satisfactory case is obtained, which shows the absolute feasibility of the ANN along with the wavelet transform. To validate the proposed method, a ±100 KV, Terminal-hybrid LCC-VSC-HVDC system is simulated via MATLAB. The outcomes verify that the proposed technique works perfectly under various fault locations, resistances, and fault types.

***doi**: 10.5829/ije.2023.34.02b.03*

1. INTRODUCTION

High-voltage direct current (HVDC) networks are extensively employed for power dispatch over long distances. There are generally two classes of HVDC systems: (i) line commutated converter-based HVDC (LCC-HVDC) systems and (ii) voltage source converter-based HVDC (VSC-HVDC) systems. The LCC-HVDC systems have such advantages as high transmission capability, long transmission extent, high transmission proficiency, and lower manufacturing costs than the latter; but the thyristors used in them are semi-controlled switches that do not have the turn-off ability. This problem has caused the LCC-HVDC systems to suffer from commutation failure for a long time and also made them unable to power a passive grid [1-3]. In contrast, VSC-HVDC systems do not experience commutation failure due to fully controlled power switches such as IGBTs and can also supply passive networks. But, compared to LCC-HVDC, they suffer from higher manufacturing costs, lower transmission efficiency, and higher losses. On the other hand, the hybrid-HVDC transmission system, which uses LCC as a rectifier and VSC as an inverter, has overcome the above problems with superiorities such as high transmission aptitude and proficiency and long transmission expanse. Besides, it does not face the problem of commutation failure and can also supply passive networks [4-7].

Recently, many fault location strategies have been suggested for HVDC systems; however, few pieces of research have been done to solve the fault location problem of LCC-VSC-HVDC transmission lines. Due to the different structures of the hybrid-HVDC systems, there would be different fault characteristics and

*Corresponding Author Institutional Email: Hadaeghi.a@shirazu.ac.ir (A. Hadaeghi)

Please cite this article as: A. Hadaeghi, M. M. Iliyaeifar, A. Abdollahi Chirani, Artificial Neural Network-based Fault Location in Terminal-hybrid High Voltage Direct Current Transmission Lines, ***International Journal of Engineering, Transactions B: Applications***, Vol. 36, No. 02, (2023), 215-225

attributes on the transmission line under various types of faults. Therefore, re-evaluation and reanalysis of the existing fault location methods are of tremendous importance, especially artificial intelligence-based strategies that have not been preached. The following are some works done in the context of hybrid HVDC systems. Wang et al. [1] offerred a traveling wave-based directional pilot protection strategy for hybrid LCC-VSC-HVDC transmission lines, in which, by dissecting the TW dispersion features alongside the HVDC transmission line and melding the instantaneous power and current on both rectifier and inverter sides, a new criterion for fault direction discrimination is presented. Wang et al. [2] suggests a directional pilot protection method based on traveling waves for hybrid LCC-MMC-HVDC transmission lines. This procedure can detect internal and external faults and does not require any particular data synchronization system. Xing et al. [8] proposed a fault localization technique for hybrid LCC-MMC-HVDC systems. In this approach, using fault attributes analysis at the rectifier station and clamp double submodule modular multilevel converter (CDSM-MMC) on the inverter station, the authors have tried to avoid the effects of transient resistance and dispersed capacitance to achieve high accuracy in fault location. Wang and Hou [9] presented a TW fault location strategy for hybrid LCC-MMC-HVDC transmission systems based on the Hilbert-Huang transform. Wang et al. [10] suggested a TW fault location method for LCC-MMC-HVDC hybrid DC transmission lines established on a capacitance-divided electronic voltage transformer (C-EVT), in which by analyzing the TW transmission characteristic of C-EVT, an algorithm is proposed based on the secondary differential voltage traveling wave (D-VTW). Wang et al. [11] presented a fault localization approach suited for hybrid HVDC systems in which the fault location is obtained based on the functional association between the fault distance and the inverter side DC bus equivalent characteristic impedance. Wang and Hou [12] offerred a traveling wave fault location method, which is established on the secondary differential current traveling wave (D-CTW) output signal of Rogowski coil electronic current transformer (R-ECT), fitting for multi-terminal hybrid LCC-MMC-HVDC transmission cables. Zhang et al. [13] deliverred a single-ended protection scenario for hybrid three-terminal LCC-VSC-HVDC systems in which internal and external faults are discovered by scrutinizing the amplitude-frequency features of the wave impedance. Gao et al. [14] suggestted a TW fault localization procedure for a hybrid three-terminal HVDC network founded on improved Local Mean Decomposition (LMD) that is not influenced by wave velocity. Wang and Zhang [15], at first, analyzed the reflection and refraction attributes of the fault traveling wave in DC buses and the defective point of LCC-MMC hybrid HVDC systems. They proposed a procedure for locating pole-to-ground and pole-to-pole faults, which does not need to detect the wave polarity and value of the wave velocity. As is common knowledge, the issue of fault localization in HVDC systems with an average error of typically more than 1% is usually debated in the majority of articles [16]. The main work of this paper is to propose and assess an artificial intelligence-based strategy for fault location in hybrid LCC-VSC-HVDC transmission lines, with the ability if locating the fault with an average percentage error of less than 1%. To do so, at first, the required voltage and current fault signals are measured from the terminals of the hybrid HVDC system. Next, wavelet transform (WT) is employed to extract high-frequency components from the input signals and improve fault location precision. Then the energy of the extracted high-frequency components is calculated and provided to the artificial neural network (ANN) as train data. Finally, the output of ANN will represent the exact location of the fault point with an accuracy of 0.0045% and 0.0943%, i.e., 22.5 and 471.5 meters from the defective spot in the lowest and highest possibilities, respectively. Additionally, it is conceivable that enhancing the DC transmission line filters will significantly reduce the average percentage error of fault location.

The remnant of this article is organized as follows. In section 2, four system-level hybrid-HVDC topologies and the theory of traveling wave-based fault location are briefly explained. In section 3, the fundamental of the utilized tools is described and given in short. In section 4, a fault location strategy based on a double-layer ANN is proposed and assessed for LCC-VSC-HVDC transmission lines. In section 5, simulations and results confirm that the offered procedure works correctly with various fault locations, fault resistances, and sorts of faults. At last, section 6 summarizes and concludes the paper.

2. LITERATURE REVIEW

In this division, four system-level hybrid HVDC topologies and traveling wave-based fault location theory will be introduced and briefly recapitulated.

2. 1. System-level Hybrid-HVDC Topologies

Xiao et al. [17] discussed four system-level hybrid-HVDC topologies in detail and resemble them in terms of DC fault ride-through strategy, PQ operating zone, and power flow reversal strategy. These four hybrid-HVDC topologies will be briefly introduced and described in this section.

2. 1. 1. Terminal-hybrid HVDC System Figure 1 depicts the basic structure of the Terminal-hybrid

HVDC topology. In this arrangement, each terminal uses a dissimilar converter. One terminal uses LCC, and the other one embraces VSC. In this topology, the VSC is usually employed on the receiving side. In this case, and due to the VSC's turn-off aptitude, it can be operated as a passive inverter, which makes it attainable to provide isolated loads without commutation failure on the receiving terminal. On the other hand, active and reactive power can be managed individually by VSC. This means the hybrid-terminal HVDC system can provide active and reactive power to intensify voltage resilience when faults appear [18].

2. 1. 2. Pole-hybrid HVDC System Figure 2 illustrates the main structure of the Pole-hybrid HVDC system. In this configuration, each terminal consists of two poles. One pole embraces LCC, and the other employs VSC, which is connected in series to assemble a bipolar arrangement. In this topology, the LCC provides part of the active power required by the system, and the rest is supplied by the VSC. The VSC is also responsible for controlling the reactive power needed for the LCC. Generally, the pole-hybrid HVDC system has high control flexibility and good dynamic performance. Furthermore, it deals with a great start-up and sufficient fault recovery. It can also be mentioned that the system can operate stably in various operating conditions [19].

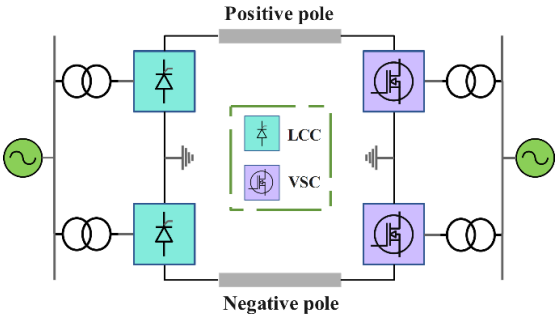

Figure 1. Main structure of the Terminal-hybrid HVDC topology

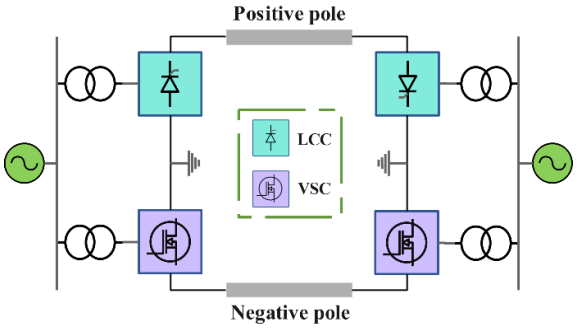

Figure 2. Main structure of the Pole-hybrid HVDC topology

2. 1. 3. Series Converter-hybrid HVDC System Figure 3 illustrates the main configuration of the series converter-hybrid HVDC system. As can be seen, in this topology, each terminal consists of several poles, each consisting of LCCs and VSCs in series connection. Due to this arrangement, the same current flows through the converters, but their voltages are different; hence their conveyed power will be disparate. The poles are also connected symmetrically to the transmission lines in this structure. Since the VSC is widely employed in rectifiers or inverter stations, the system deals with flexible active and reactive power management. Furthermore, due to the control collaboration between the LCC and VSC, there would not be any current cut-off under AC faults on the rectifier side. Besides, if an AC fault arises on the inverter side, the transmitted power can be preserved to some extent [20].

2. 1. 4. Parallel Converter-hybrid HVDC System Figure 4 shows the rudimentary arrangement of the Parallel converter-hybrid HVDC system. Each terminal

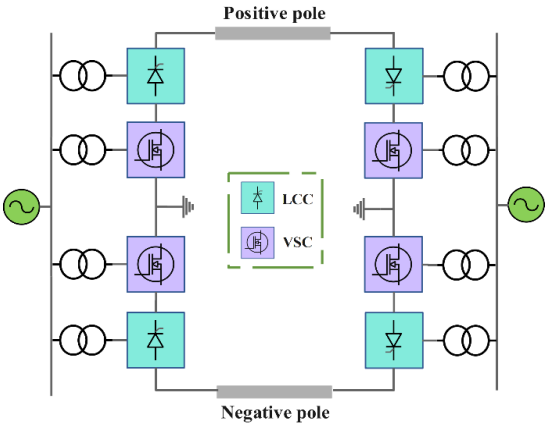

Figure 3. Main structure of the Series converter-hybrid HVDC topology

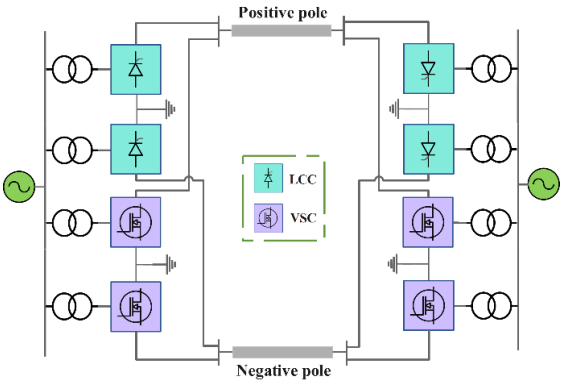

Figure 4. Main structure of the Parallel converter-hybrid HVDC topology

is composed of LCCs and VSCs connected in parallel in this topology. As can be seen, both LCC and VSC portion an identical transmission line and retain equal DC voltage, but the flowing current is different; hence, they provide dissimilar power ratings. Overall, this topology has many potentials, such as bulk-power transmission capability, power reversal capability, reactive power compensation, and fault ride-through ability. Furthermore, if either LCCs or VSCs are halted, the rest of the system can operate smoothly without any problem [21].

2. 2. Travelling Wave-based Fault Location Theory

When a fault appears in a power system transmission line, the traveling waves propagate along the line in the form of electromagnetic pulses in both directions from the fault point to the system terminals. These waves spread along the line and experience reflections and refractions as they propagate. Then the energy of these traveling waves is gradually reduced according to the fault and system characteristics until it is completely dissipated [22]. These waves contain information about the fault, including its location and its distance from the system terminals, which can be used to detect and locate the faulty point. By accurately measuring the arrival time and propagation speed of two consecutive peaks of these traveling waves that are heading to the system's terminals, the exact location of the faulty point can be determined.

The following partial differential equations pertain to the voltage and current measurements taken at any point x:

$$\frac{\partial e}{\partial x} = -L\frac{\partial \mathrm{i}}{\partial \mathrm{t}} \quad \text{and} \quad \frac{\partial \mathrm{i}}{\partial x} = -C\frac{\partial e}{\partial t} \tag{1}$$

where L and C represent the line's inductance and capacitance, respectively, for each unit of the line's length. It is presumed that there will be a negligible amount of resistance. These equations have the following answers as their solutions:

$$e(x,t) = e_f(x - vt) + e_r(x + vt) \tag{2}$$

$$i(x,t) = \frac{1}{z}e_f(x - vt) - \frac{1}{z}e_r(x + vt) \tag{3}$$

where $Z = \sqrt{(L/C)}$ denotes the transmission line characteristic impedance and $V = 1/\sqrt{(LC)}$ indicates the velocity at which the signal is propagating. Both forward (e_f and i_f) and backward (e_r and i_r) waves, as shown in Figure 5, depart the disturbed area "x" heading in various directions at the speed of "v," which is a tiny bit smaller than the light speed, toward the transmission line extremities. The terminations of transmission lines constitute a discontinuity or a change in impedance, and as a result, some of the wave's energy will be reflected back to the source of the disturbance. The remainder of the power will be distributed across the system via

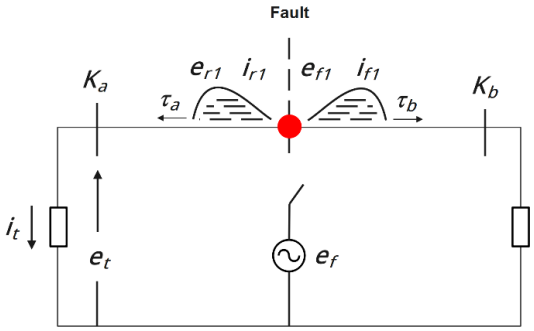

Figure 5. Voltage and current traveling waves

transmission lines or other power system components. Figure 6 depicts the numerous waves created at the ends of the line using a Bewley Lattice diagram. Reflection coefficients k_a and k_b, which are based on characteristic impedance ratios at the discontinuities, are used to express the amplitudes of waves. Time intervals, τ_α and τ_b, are used to illustrate how much time it takes for a fault to reach the discontinuity point. The distance (x) from substation A to the defective point can be determined by just using the line length (l) and the duration of the arrival discrepancy ($\tau_\alpha - \tau_b$) as follows:

$$x = \frac{1 - c(\tau_\alpha - \tau_b)}{2} \tag{4}$$

In Equation (4), C denotes the wave propagation of 299.79 μm/μsec (≅1ft/ns) [23].

3. FUNDAMENTALS OF THE UTILIZED TOOLS

This part will briefly explain the basic principles of the utilized implements, including wavelet transforms and artificial neural networks.

3. 1. Artificial Neural Network

Artificial neural networks (ANNs) are conventional machine learning

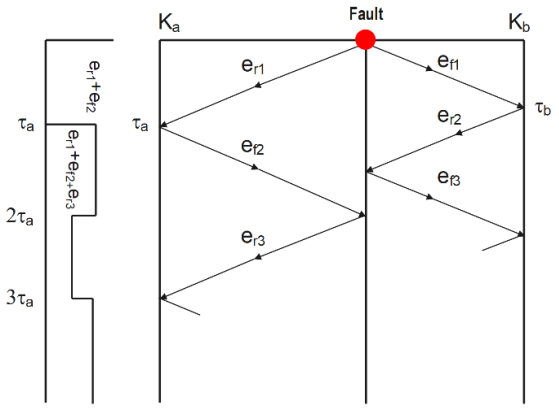

Figure 6. Bewley Lattice Diagram

strategies that simulate the learning mechanism of the human brain. ANN is a new way to predict and model time series that are not linear and can't be solved easily or accurately [24, 25].

Artificial neural networks are generally divided into two categories: (i) single-layer neural networks and (ii) multilayer neural networks. A single-layer neural network is the simplest type of neural network that consists of an input layer and an output node. In this network, data is transferred directly from the input layer to the output layer, and all operations are visible to the user. This network is also called a perceptron. Figure 7(a) shows a single-layer neural network. A multilayer neural network, on the other hand, has multiple computational layers in which neurons are arranged in a layered structure. In this network, the input and output layers are split by a group of layers called "hidden layers," as their executed operations are not visible to the user. Multilayer neural networks are also referred to as feed-forward networks [26, 27]. Figure 7(b) illustrates a multilayer neural network.

ANN is generally a fast and accurate method for fault localization. One of the most prominent features of ANN is that its process follows a very simple set of operations. Typically, in a power system, the values of voltage and current are very unstable and change under various types of faults. Hence, an artificial neural network would be a great choice for detecting, classifying, and locating the transmission line faults of HVDC systems, as a neural network is basically able to incorporate dynamic changes in power systems [28-32].

3. 2. Wavelet Transform Processing non-static signals is difficult and requires specific tools for analysis. Nowadays, the wavelet transform is widely employed in the field of transmission line fault localization in HVDC systems due to its high ability for fault transient analysis as discussed in literature [33-36]. In this paper, the wavelet transform is utilized in order to improve fault location accuracy as well as extract high-frequency components from the input voltage and current fault signals.

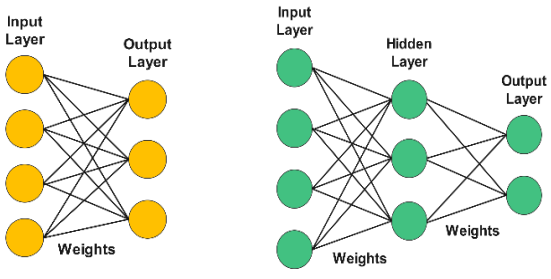

(a) (b)

Figure 7. The architecture of neural networks. (a) single-layer neural network. (b) multilayer neural network

In general, the wavelet transform of a function *v(t)* can be defined as the following relationship [37]:

$$WT_{\psi(a.b)}v(t) = \int_{-\infty}^{+\infty} V(t)\Psi^*_{a.b}(t)dt \quad (5)$$

where $\Psi^*_{a.b}(t)$ is the daughter wavelet and is defined as follows:

$$\Psi^*_{a.b}(t) = \frac{1}{\sqrt{\alpha}}\Psi(\frac{t-b}{a}) \quad (6)$$

In Equation (6), α is the binary dilation and is responsible to scale the mother wavelet $\psi_{a.b}(t)$. b is the binary position by which the mother wavelet is translated (shifted). The daughter wavelet is indeed a translated and dilated version of the mother wavelet [38, 39].

Wavelet transforms can generally be divided into two categories: (i) continuous wavelet transform (CWT) and (ii) discrete wavelet transform (DWT). Basically, CWT detects wave time more accurately than DWT, but DWT is computationally faster and considered by researchers to be more suitable for protective applications.

In this paper, as mentioned before, the wavelet transform has been utilized in order to extract high-frequency components from fault signals as well as to increase fault location accuracy. There are several mother wavelets that can be used in the proposed method, including Haar, Daubechies, Symlets, Biorthogonal, etc. In this paper, the Daubechies mother wavelet (db4) is employed to decompose fault signals into 15 levels. The simulation results confirm that the 15-level decomposition has the best outcome among the selected levels for WT in the proposed algorithm.

4. THE PROPOSED METHOD

Due to their high proficiency in pattern detection and classification, artificial neural networks are considered an excellent apparatus for the localization of faults in power transmission lines. In this paper, an artificial neural network is employed to locate the transmission line fault of the studied Terminal-hybrid LCC-VSC-HVDC system. For this purpose, the Levenberg-Marquardt backpropagation algorithm (trainlm) has been hired as the train function in MATLAB software. Besides, according to Equation (7), the hyperbolic tangent sigmoid transfer function (tansig) is employed for the input and hidden layers, and the linear transfer function (purlin) is utilized for the output layer.

$$tansig(s) = \frac{2}{1+e^{-2s}} - 1 \quad (7)$$

In addition, 70% of the total input data is considered training data, 15% validation data, and 15% test data. Finally, in order to evaluate the network performance according to Equation (8), the mean squared normalized error performance function (MSE) is exploited. It can also be noted that the single input data, which are a total

of eight different types of signals, are employed as intake data.

$$MSE = \frac{1}{n}\sum_{i=1}^{n}(Y_i - \hat{Y}_i)^2 \quad (8)$$

where n is the number of data points and Y_i and $\hat{Y}_i$ represent the observed and predicted values, respectively. The closer the MSE value is to zero, the more accurately the artificial neural network can specify the fault location.

To obtain the train patterns needed for the artificial neural network, all types of faults, including positive pole to ground (PG), negative pole to ground (NG), positive pole to negative pole (PN), and positive pole to negative pole to ground (PNG), are applied to 500 different points along the entire DC transmission line with varying fault resistances (0.1, 1, 20, 70, and 100 Ω). The fault distance starts at 0.5 km from the rectifier terminal and continues with a step of 1 km to a distance of 499.5 km from the same terminal. The duration of the fault is also set to be 20 milliseconds. It is to be mentioned that, in this stage, a total of 10000 samples (4 types of faults × 5 individual fault resistances × 500 different points) are collected from the terminals of the employed Terminal-hybrid LCC-VSC-HVDC system to verify the proposed fault location strategy. Then, using the wavelet transform, the high-frequency components of these 10000 samples are extracted into 15 levels. Furthermore, in order to obtain the required test data, all four types of faults (PG, NG, PN, and PNG) with fault resistances of (2, 5, 25, 80, and 120 Ω) were applied to 50 random points throughout the entire length of the DC transmission line. Then, like the train data, the high-frequency components of test data are also decomposed into 15 levels by the use of wavelet transform. It has to be noted that, the Daubechies mother wavelet of type (db4) is indeed employed in order to increase the fault localization preciseness as well as to extract high-frequency components from the train and test fault signals. In the next step, according to Equation (9), the energy of all 15 levels of the decomposed high-frequency components of both train and test signals will be calculated and given to a double-layer artificial neural network as intake data. To do this, a double-layer artificial neural network with 20 neurons in the first hidden layer and 4 neurons in the second hidden layer is adopted. Finally, according to Equation (10), the output of ANN will determine the exact location of the faulty point with an average percentage error of about 0.0045%, which is a distance of 22.5 meter from defective spot. The flowchart of the main steps of the evaluated fault location method is shown in Figure 8.

$$E_{X_n} = \int_{t_1}^{t_1+\Delta t} X_n^2(t)dt \quad (9)$$

$$\text{percentage error (\%)} = \frac{|X_1 - X_2|}{\text{L}} \times 100 \quad (10)$$

In Equation (9), t_1 and Δt stand for the start time and the length of the sampling window, while n stands for the level of data decomposition. In Equation (10), X_1 and X_2 represent the actual fault location and the estimated fault location, respectively, while L stands for the total length of the transmission line.

5. SIMULATION AND RESULTS

5. 1. System Specification The structure of the exerted hybrid HVDC system is depicted in Figure 9. In order to test and validate the proposed algorithm, a Terminal-hybrid LCC-VSC-HVDC system is implemented and simulated by MATLAB software. In this topology, the rectifier side uses a twelve-pulse LCC, and the inverter side adopts a conventional two-level VSC. Besides, The SPWM control strategy is used for the VSC side. The switching frequency is also set to be 10 kHz. The main specifications of the utilized system are listed in Table 1.

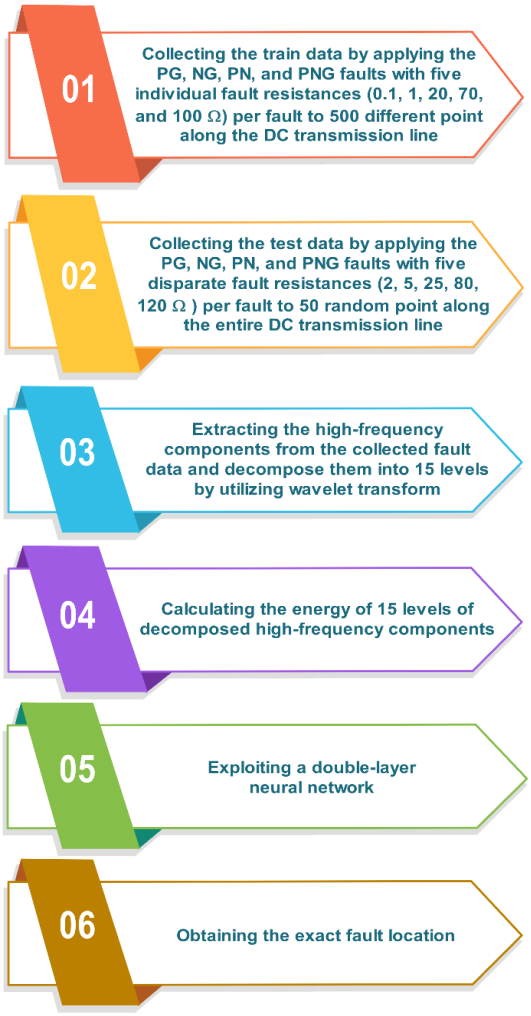

Figure 8. The flowchart of the proposed fault location method's principal steps

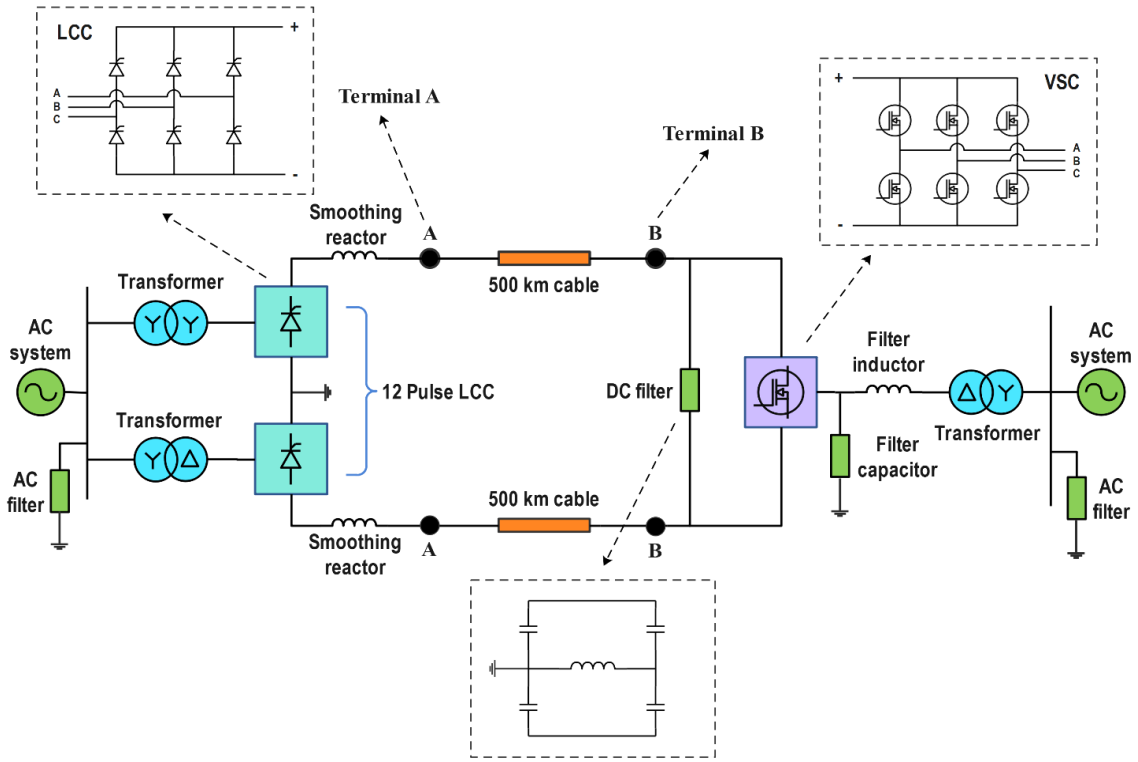

Figure 9. The main configuration of the utilized Terminal-hybrid LCC-VSC-HVDC system

TABLE 1. The main specification of the Terminal-hybrid LCC-VSC-HVDC system

Real power (P)	1100 MW
AC voltage	230 kV
Nominal frequency	50 Hz
Transmission line DC voltage (v_{dc})	±100 kV
Transmission line DC current (i_{dc})	2 kA
Cable length	500 km
Cable resistance	0.0139 Ω/km
Cable inductance	0.159 mH/km
Cable capacitance	231 nF/km

5. 2. Fault Location Results Using a Double-layer Artificial Neural Network In this paper, a total of eight measuring probes are embedded to gauge the transmission line voltage and current signals during the fault circumstance, which includes rectifier side (terminal A), positive pole current (IP1), negative pole current (IN1), positive pole to ground voltage (VP1), negative pole to ground voltage (VN1), and inverter side (terminal B) positive pole current (IP2), negative pole current (IN2), positive pole to ground voltage (VP2), and negative pole to ground voltage (VN2). Furthermore, a double-layer artificial neural network is exploited to achieve the best network performance with 20 and 4 neurons for the first and second hidden layers, respectively. According to Equation (10), the average percentage error of fault location using a double-layer artificial neural network under 4 different types of faults with 5 disparate fault resistances (0.1, 1, 20, 70, and 100 Ω for train data) and (2, 5, 25, 80, and 120 Ω for test data) based on both the type of fault and the type of signal along with the graph are displayed in Table 2, Figures 10 and 11, respectively.

Moreover, in order to prove the sufficiency of the selected levels for wavelet transform decomposition, 5 different levels, including 5, 10, 15, 20, and 25, have been chosen to be analyzed. The test was performed under the PG fault type with the same fault resistances (0.1, 1, 20, 70, and 100 Ω for train data) and (2, 5, 25, 80, and 120 Ω for test data). Besides, the same double-layer neural network was employed with 20 and 4 neurons for the first and second hidden layers, respectively. The experimental results are shown in Table 3 and Figure 12, respectively. The results indicate that the 5-level decomposition eventually culminated in a far less beneficial outcome, and this can be seen to be the case right off the bat. However, as the number of levels of decomposition is increased, the results continue to get better and better until they reach a point where they converge relatively around the 15-level decomposition. As a matter of fact, 15-level decomposition has the best result among the selected levels for the wavelet transform.

TABLE 2. The average percentage error of fault location using a double-layer ANN with the number of neurons [20 4] in the hidden layers under four different types of faults and five particular fault resistances

Type of data	Type of fault				Average percentage error (%)
	PG	NG	PN	PNG	
IP1	0.0024	0.0003	0.0115	0.0121	**0.0066**
IN1	0.0008	0.0028	0.0074	0.0069	**0.0045**
VP1	0.0323	0.0083	0.1660	0.1104	**0.0544**
VN1	0.0068	0.0248	0.1639	0.1705	**0.0915**
IP2	0.0319	0.0037	0.0916	0.0679	**0.0488**
IN2	0.0038	0.0267	0.0820	0.0835	**0.0490**
VP2	0.0164	0.0065	0.1797	0.1533	**0.0890**
VN2	0.0061	0.0172	0.1530	0.2009	**0.0943**
Average percentage error (%)	**0.0126**	**0.0113**	**0.1069**	**0.1007**	

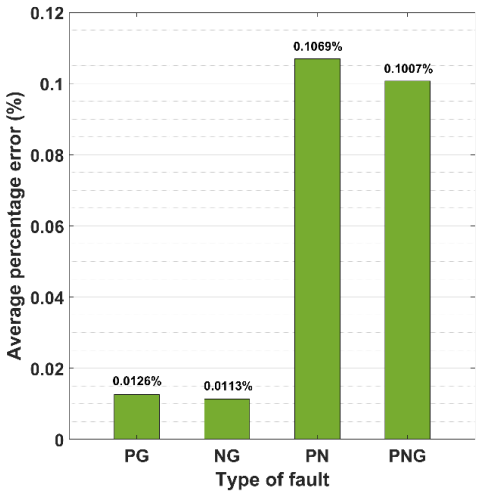

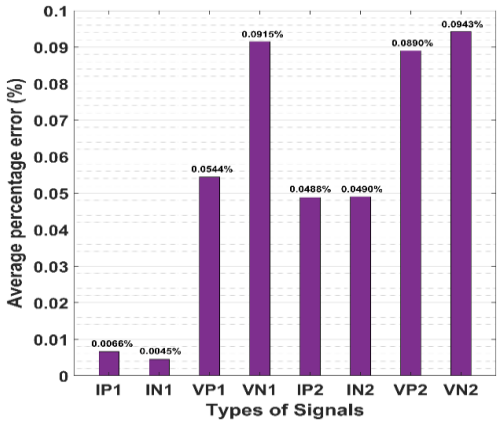

Figure 10. The average percentage error of fault location using a double-layer ANN with the number of neurons [20 4] in the hidden layers and five particular fault resistances based on different types of faults

TABLE 3. The average percentage error of fault location using different decomposition levels of the wavelet transform under the PG fault type and five disparate fault resistances

Type of data	Levels of decomposition				
	5	10	15	20	25
IP1	0.2891	0.1407	0.0024	0.0062	0.0037
IN1	0.0146	0.0034	0.0008	0.0018	0.0075
VP1	0.7877	0.1949	0.0323	0.1139	0.0918
VN1	0.9161	0.2412	0.0068	0.0447	0.0457
IP2	0.7605	0.2103	0.0319	0.0354	0.0618
IN2	0.3728	0.1260	0.0038	0.0092	0.0955
VP2	0.6975	0.1755	0.0164	0.1070	0.2095
VN2	0.4393	0.2244	0.0061	0.0554	0.2024
Average percentage error (%)	**0.5347**	**0.1646**	**0.0126**	**0.0467**	**0.0897**

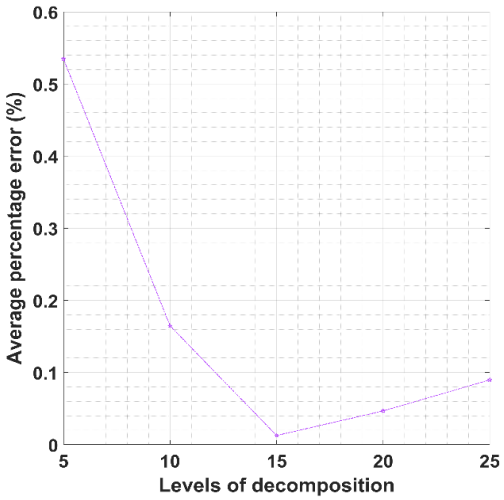

Figure 11. The average percentage error of fault location using a double-layer ANN with the number of neurons [20 4] in the hidden layers and five particular fault resistances based on different types of signals

As can be inferred from Table 2 and Figure 11, the proposed fault location algorithm using the positive and negative pole current signals of the rectifier side (IP1 and IN1) has the best results among others. It can be seen that PN and PNG fault localization using positive and negative pole currents of the inverter side (IP2 and IN2) as well as positive and negative pole to ground voltages of both sides (VP1, VN1, VP2, and VN2) have a notably higher error rate than the two aforementioned signals. The fact that there are two large smoothing reactors in the rectifier terminal would be the only reason that can be taken into account, since they basically prevent sharp pulses and sudden changes in the current when a fault emerges, hence making it more appropriate for the rectifier side positive and negative pole current signals (IP1 and IN1) to be effectively used for transmission line fault localization of the utilized Terminal-hybrid LCC-VSC-HVDC system.

Because of the symmetrical nature of the system's terminals and the use of the same kind of converter on both ends of the transmission line, identical DC filters are utilized on both sides of the transmission line in tradditional high-voltage direct current (HVDC) systems, as is common knowledge. On the other hand, the Terminal-hybrid HVDC system incorporates disparate filters with various values on both ends due to the presence of two different types of converters on both substations. In addition, any increase in the value of the DC transmission line capacitor filters on the inverter side (VSC), will result in a considerable rise in the amount of time required for the transmission line voltages and currents to transition from one state to another. As a result, capacitor filters with an average value of roughly 70μF are implemented in this research for the VSC side transmission line in order to circumvent the problem with the transient period. On the rectifier side (LCC), in contrast, there are two huge smoothing reactors each with a value of 200mH. Because of such a preference, the fault currents of the positive and negative poles of the rectifier side (LCC) (IP1 and IN1) were kept to a minimum, which significantly reduced the potential of sharp pulses and rapid changes occurring during the fault scenario. Over this, the process of learning of the artificial neural network has been drastically enhanced. Correspondingly, the positive and negative pole currents of the rectifier side (IN1 and IP1) have become more appropriate for the fault location of the employed Terminal-hybrid LCC-VSC-HVDC transmission system. Therefore, the transmission line failures of Terminal-hybrid LCC-VSC-HVDC networks may be satisfactorily identified through the utilization of these two signals, all of which were described earlier in the argument. It is possible to draw the conclusion that by designing appropriate DC filters to be installed on the DC Power line, not only is it possible to alleviate the ripple voltage and current of the HVDC transmission line as well as enhance the reliability of the conveyed power, but it is also feasible to efficiently expedite the fault location problem in a way that is both surprising and novel.

6. CONCLUSION

This paper uses artificial neural network to evaluate the transmission line fault location issue of Terminal-hybrid LCC-VSC-HVDC systems. To do so, all types of faults, including PG, NG, PN and PNG faults with 5 individual fault resistances (0.1, 1, 20, 70, and 100 Ω for train data) and (2, 5, 25, 80, and 120 Ω for test data) are applied to 500 different points along the DC transmission line and voltage and current fault signals are measured from the hybrid system terminals. These signals are then decomposed and their high frequency components are extracted to 15 levels by the use of wavelet transform. In the next step, the energy of all 15 levels of the extracted high-frequency components is calculated and provided to a double-layer artificial neural network with neurons in the hidden layers as input train and test data. Finally, the exact location of the fault is determined by using the artificial neural network.

As a result of this research, the average percentage error was found to have a value of 0.0045%, which corresponds to a range of 22.5 meters from the faulty spot in the most sufficient scenario. This demonstrates that the ANN, in conjunction with the wavelet transform, is utterly feasible in the field of fault localization in hybrid-HVDC networks. According to the simulation results and

due to the different structure of the studied Terminal-hybrid LCC-VSC-HVSC system in compare to conventional HVDC systems (LCC-HVDC and VSC-HVDC) and also the use of two large smoothing reactors on the rectifier side, it can be observed that the positive and negative pole current signals of the rectifier side (IP1 and IN1) achieve the best results in the proposed fault location algorithm. In other words, it is best to understand the significance of the role that DC filters play throughout the transmission line of HVDC networks and the influence that they already have in terms of fault location. It is undeniable that a well-designed DC filter for the DC transmission line can ameliorate the ripple voltage and current of the HVDC transmission line, enhance the integrity of the power being transferred, and significantly mitigate the fault location difficulties. Hence, the authors will suggest the use of the two aforementioned signals for transmission line fault localization in Terminal-hybrid LCC-VSC-HVDC systems.

7. REFERENCES

1. Wang, D., Hou, M., Gao, M. and Qiao, F., "Travelling wave directional pilot protection for hybrid hvdc transmission line", ***International Journal of Electrical Power & Energy Systems***, Vol. 107, (2019), 615-627. doi: 10.1016/j.ijepes.2018.12.028
2. Wang, D., Hou, M., Gao, M. and Qiao, F., "Travelling wave directional pilot protection for hybrid lcc-mmc-hvdc transmission line", ***International Journal of Electrical Power & Energy Systems***, Vol. 115, (2020), 105431. doi: 10.1016/j.ijepes.2019.105431
3. Zare, H., Khanalizadeh Eini, M. and Esmaeili, A., "Stabilization of voltage and current in the distribution networks using apf and tsc", ***International Journal of Engineering, Transactions B: Applications***, Vol. 35, No. 5, (2022), 1064-1073. doi: 10.5829/IJE.2022.35.05B.21
4. Xiao, H., Xu, Z., Tang, G. and Xue, Y., "Complete mathematical model derivation for modular multilevel converter based on successive approximation approach", ***IET Power Electronics***, Vol. 8, No. 12, (2015), 2396-2410. doi: 10.1049/iet-pel.2014.0892
5. Farshad, M. and Karimi, M., "Intelligent protection of csc-hvdc lines based on moving average and maximum coordinate difference criteria", ***Electric Power Systems Research***, Vol. 199, (2021), 107439. doi: 10.1016/j.epsr.2021.107439
6. Tavassoli, F., Ghoreishy, H., Adabi, J. and Rezanejad, M., "An advanced modulation technique featuring common mode voltage suppression for three-phase neutral point clamped back to back converters", ***International Journal of Engineering, Transactions B: Applications***, Vol. 35, No. 11, (2022), 2220-2228. doi: 10.5829/IJE.2022.35.11B.17
7. Abbasghorbani, M., "Prioritization of transmission network components based on their failure impact on reliability of composite power systems", ***International Journal of Engineering, Transactions C: Aspects***, Vol. 35, No. 3, (2022), 502-509. doi: 10.5829/IJE.2022.35.03C.02
8. Xing, C., Li, S. and Xi, X., "Research on a fault location method for a pole-to-pole short-circuit fault in an lcc-mmc hybrid dc transmission system", ***IEEE Access***, Vol. 8, (2020), 165683-165692. doi: 10.1109/ACCESS.2020.3022717
9. Wang, D. and Hou, M., "Travelling wave fault location algorithm for lcc-mmc-mtdc hybrid transmission system based on hilbert-huang transform", ***International Journal of Electrical Power & Energy Systems***, Vol. 121, (2020), 106125. doi: 10.1016/j.ijepes.2020.106125
10. Wang, D., Yang, H., Hou, M. and Guo, Y., "Travelling wave fault location principle for hybrid multi-terminal lcc-mmc-hvdc transmission lines based on c-evt", ***Electric Power Systems Research***, Vol. 185, (2020), 106402. doi: 10.1016/j.epsr.2020.106402
11. Wang, J., Zhang, Y. and Li, T., "Equivalent characteristic impedance based hybrid-hvdc transmission line fault location", ***Electric Power Systems Research***, Vol. 194, (2021), 107055. doi: 10.1016/j.epsr.2021.107055
12. Wang, D. and Hou, M., "Travelling wave fault location principle for hybrid multi-terminal lcc-vsc-hvdc transmission line based on r-ect", ***International Journal of Electrical Power & Energy Systems***, Vol. 117, (2020), 105627. doi: 10.1016/j.ijepes.2019.105627
13. Zhang, D., Wu, C., He, J. and Liang, C., "A new protection scheme for transmission line of three-terminal hybrid hvdc system", ***International Journal of Electrical Power & Energy Systems***, Vol. 134, (2022), 107446. doi: 10.1016/j.ijepes.2021.107446
14. Gao, S., Xu, Z., Song, G., Shao, M. and Jiang, Y., "Fault location of hybrid three-terminal hvdc transmission line based on improved lmd", ***Electric Power Systems Research***, Vol. 201, (2021), 107550. doi: 10.1016/j.epsr.2021.107550
15. Wang, J. and Zhang, Y., "Traveling wave propagation characteristic-based lcc-mmc hybrid hvdc transmission line fault location method", ***IEEE Transactions on Power Delivery***, (2021). doi: 10.1109/TPWRD.2021.3055840
16. Roy, N.B., "Fault identification and determination of its location in a hvdc system based on feature extraction and artificial neural network", ***Journal of The Institution of Engineers (India): Series B***, Vol. 102, No. 2, (2021), 351-361. doi: 10.1007/s40031-021-00541-5
17. Xiao, H., Sun, K., Pan, J., Li, Y. and Liu, Y., "Review of hybrid hvdc systems combining line communicated converter and voltage source converter", ***International Journal of Electrical Power & Energy Systems***, Vol. 129, (2021), 106713. doi: 10.1016/j.ijepes.2020.106713
18. Li, G., Li, G., Liang, H., Yin, M. and Zhao, C., "Operational mechanism and characteristic analysis of novel hybrid hvdc system", in 2006 International Conference on Power System Technology, IEEE., (2006), 1-6. doi: 10.1109/ICPST.2006.321914
19. Qahraman, B. and Gole, A., "A vsc based series hybrid converter for hvdc transmission", in Canadian Conference on Electrical and Computer Engineering, 2005., IEEE., (2005), 458-461. doi: 10.1109/CCECE.2005.1556970
20. Xu, Z., Wang, S. and Xiao, H., "Hybrid high-voltage direct current topology with line commutated converter and modular multilevel converter in series connection suitable for bulk power overhead line transmission", ***IET Power Electronics***, Vol. 9, No. 12, (2016), 2307-2317. doi: 10.1049/iet-pel.2015.0738
21. Xiao, H., Sun, K., Pan, J. and Liu, Y., "Operation and control of hybrid hvdc system with lcc and full-bridge mmc connected in parallel", ***IET Generation, Transmission & Distribution***, Vol. 14, No. 7, (2020), 1344-1352. doi: 10.1049/iet-gtd.2019.1336
22. Wijaya, G. and Abu-Siada, A., "Review of transmission line fault location using travelling wave method", in 2018 Conference on Power Engineering and Renewable Energy (ICPERE), IEEE., (2018), 1-6. doi: 10.1109/ICPERE.2018.8739752
23. Packard, H., "Traveling wave fault location in power transmission systems", ***Application Note***, Vol. 1285, (1997).

24. Hadaeghi, A., Samet, H. and Ghanbari, T., "Multi extreme learning machine approach for fault location in multi-terminal high-voltage direct current systems", ***Computers & Electrical Engineering***, Vol. 78, (2019), 313-327. doi: 10.1016/j.compeleceng.2019.07.022
25. Abderrazak, L., Hanane, K.S., Adlene, R., Mohamed, A. and Mohamed, K., "Fuzzy logic control of mppt controller in autonomous hybrid power generation system by using extended kalman filter for battery soc estimation", ***International Journal of Engineering, Transactions B: Applications***, Vol. 36, No. 2, (2023).
26. Aggarwal, C.C., "Neural networks and deep learning", ***Springer***, Vol. 10, (2018), 978-973. doi: 10.1007/978-3-319-94463-0
27. Tzelepis, D., Mirsaeidi, S., Dyśko, A., Hong, Q., He, J. and Booth, C.D., "Intelligent fault location in mtdc networks by recognizing patterns in hybrid circuit breaker currents during fault clearance process", ***IEEE Transactions on Industrial Informatics***, Vol. 17, No. 5, (2020), 3056-3068. doi: 10.1109/TII.2020.3003476
28. Nagar, K. and Shah, M., "A review on different ann based fault detection techniques for hvdc systems", I***nternational Journal of Innovative Research in Engineering & Management***, Vol. 3, No. 6, (2016), 477-481. doi: 10.21276/ijirem.2016.3.6.5
29. Hussain, M., Dhimish, M., Titarenko, S. and Mather, P., "Artificial neural network based photovoltaic fault detection algorithm integrating two bi-directional input parameters", ***Renewable Energy***, Vol. 155, (2020), 1272-1292. doi: 10.1016/j.renene.2020.04.023
30. Ankar, S. and Yadav, A., "Wavelet-ann based fault location scheme for bipolar csc-based hvdc transmission system", in 2020 First International Conference on Power, Control and Computing Technologies (ICPC2T), IEEE., (2020), 85-90. doi: 10.1109/ICPC2T48082.2020.9071450
31. Xiang, W., Yang, S. and Wen, J., "Ann-based robust dc fault protection algorithm for mmc high-voltage direct current grids", ***IET Renewable Power Generation***, Vol. 14, No. 2, (2020), 199-210. doi: 10.1049/iet-rpg.2019.0733
32. Khan, N.M., Mansoor, M., Moosavi, S.K.R., Zafar, M.H., Khan, U.A. and Shahzad, M., "A novel search and rescue optimization algorithm based artificial neural network for identification, classification and location of dc fault in two terminal hvdc transmission systems", in 2022 International Conference on Emerging Trends in Smart Technologies (ICETST), IEEE. (2022), 1-6. doi: 10.1109/ICETST55735.2022.9922910
33. Ye, X., Lan, S., Xiao, S.j. and Yuan, Y., "Single pole-to-ground fault location method for mmc-hvdc system using wavelet decomposition and dbn", ***IEEJ Transactions on Electrical and Electronic Engineering***, Vol. 16, No. 2, (2021), 238-247. doi: 10.1002/tee.23290
34. Ravesh, N.R., Ramezani, N., Ahmadi, I. and Nouri, H., "A hybrid artificial neural network and wavelet packet transform approach for fault location in hybrid transmission lines", ***Electric Power Systems Research***, Vol. 204, (2022), 107721. doi: 10.1016/j.epsr.2021.107721
35. Rohani, R., Koochaki, A. and Siahbalaee, J., "Fault location in vsc-hvdc systems based on nsga-ii and discrete wavelet transform", ***International Journal of Renewable Energy Research (IJRER)***, Vol. 12, No. 3, (2022), 1347-1361. doi: 10.20508/ijrer.v12i3.13050.g8519
36. Yi, L., Liu, Y., Lu, D., Nie, Y. and Zheng, X., "Hvdc line fault location using wavelets to mitigate impact of frequency dependent line parameters", in 2022 IEEE Power & Energy Society General Meeting (PESGM), IEEE., (2022), 1-5. doi: 10.1109/PESGM48719.2022.9916742
37. Hadaeghi, A., Samet, H. and Ghanbari, T., "Multi svr approach for fault location in multi-terminal hvdc systems", ***International Journal of Renewable Energy Research (IJRER)***, Vol. 9, No. 1, (2019), 194-206. doi: 10.20508/ijrer.v9i1.8868.g7576
38. Tzelepis, D., Dyśko, A., Fusiek, G., Niewczas, P., Mirsaeidi, S., Booth, C. and Dong, X., "Advanced fault location in mtdc networks utilising optically-multiplexed current measurements and machine learning approach", ***International Journal of Electrical Power & Energy Systems***, Vol. 97, (2018), 319-333. doi: 10.1016/j.ijepes.2017.10.040
39. Pourafzal, A., Fereidunian, A. and Safarihamid, K., "Chaotic time series recognition: A deep learning model inspired by complex systems characteristics", ***International Journal of Engineering, Transactions A: Basics***, Vol. 36, No. 1, (2023). doi: 10.5829/IJE.2023.36.01A.01

Persian Abstract

چکیده

در این مقاله، یک تکنیک مکان‌یابی خطا براساس شبکهٔ عصبی مصنوعی (ANN) برای سیستمهای HVDC هایبریدی-ترمینالی از نوع LCC-VSC-HVDC مورد بررسی و ارزیابی قرار گرفته است. در سیستم‌های HVDC متداول (سیستمهای HVDC مبتنی بر LCC و یا مبتنی بر VSC)، به دلیل استفاده از مبدل‌های مشابه در پایانه‌های فرستنده و گیرنده، از فیلترهای یکسان در هر دو سمت خط انتقال استفاده می‌گردد. در این مقاله نتیجه گرفته می‌شود که با توجه به استفاده از دو نوع مبدل مختلف در هر دو انتهای سیستم هایبریدی-ترمینالی مورد استفاده از نوع LCC-VSC-HVDC و استفاده از فیلترهای DC مختلف در هر دو طرف، مکان‌یابی خطا با استفاده از جریان‌های قطب مثبت و منفی سمت یکسوساز نتایج بسیار بهتری نسبت به بقیه سیگنال‌های ورودی خواهد داشت. بنابراین، مشخص خواهد شد که با افزایش و طراحی فیلترهای DC مناسب بر روی خط انتقال سیستم‌های HVDC هایبریدی، مسالهٔ مکان‌یابی خطا به طور قابل‌توجه و شگفت انگیزی تسهیل خواهد یافت. امروزه مکان‌یابی خطا در خطوط انتقال HVDC با مقداری بیش از ۱ ٪ به طور کلی در اکثر مقالات مورد بحث قرار می‌گیرد. در این تحقیق، مکان دقیق خطا با مقدار ۰.۰۰۴۵ ٪ یعنی فاصلهٔ ۲۲.۵ متری از نقطهٔ خطا در رضایتبخش‌ترین حالت بدست آمده است که عملکرد بی‌نظیر شبکهٔ عصبی مصنوعی را در کنار تبدیل موجک نمایش می‌دهد. به منظوراعتبارسنجی روش پیشنهادی، یک سیستم هایبریدی-ترمینالی از نوع LCC-VSC-HVDC از طریق نرم‌افزار MATLAB شبیه‌سازی شده است. نتایج تایید می‌کنند که روش پیشنهادی به طور کامل تحت موقعیت‌های مختلف، مقاومت‌های مختلف و انواع متفاوت خطا به درستی عمل می‌کند.